

Morphological Change and Cell Disruption of *Haematococcus pluvialis* Cyst during High-Pressure Homogenization for Astaxanthin Recovery

Praveenkumar, Ramasamy; Lee, Jiye; Vijayan, Durairaj; Lee, Soo Youn; Lee, Kyubock; Sim, Sang Jun; Hong, Min Eui; Kim, Young-Eun; Oh, You-Kwan

Published in:
Applied Sciences

DOI:
[10.3390/app10020513](https://doi.org/10.3390/app10020513)

Publication date:
2020

Document Version
Publisher's PDF, also known as Version of record

Citation for published version (APA):
Praveenkumar, R., Lee, J., Vijayan, D., Lee, S. Y., Lee, K., Sim, S. J., Hong, M. E., Kim, Y.-E., & Oh, Y.-K. (2020). Morphological Change and Cell Disruption of *Haematococcus pluvialis* Cyst during High-Pressure Homogenization for Astaxanthin Recovery. *Applied Sciences*, 10(2), Article 513.
<https://doi.org/10.3390/app10020513>

General rights

Copyright and moral rights for the publications made accessible in the public portal are retained by the authors and/or other copyright owners and it is a condition of accessing publications that users recognise and abide by the legal requirements associated with these rights.


- Users may download and print one copy of any publication from the public portal for the purpose of private study or research.
- You may not further distribute the material or use it for any profit-making activity or commercial gain.
- You may freely distribute the URL identifying the publication in the public portal.

Take down policy

If you believe that this document breaches copyright please contact rucforsk@kb.dk providing details, and we will remove access to the work immediately and investigate your claim.

Article

Morphological Change and Cell Disruption of *Haematococcus pluvialis* Cyst during High-Pressure Homogenization for Astaxanthin Recovery

Ramasamy Praveenkumar ^{1,2} , Jiye Lee ³, Durairaj Vijayan ³ , Soo Youn Lee ³, Kyubock Lee ⁴, Sang Jun Sim ⁵ , Min Eui Hong ⁵, Young-Eun Kim ⁶ and You-Kwan Oh ^{6,*} 

¹ Department of Science and Environment, Roskilde University, 4000 Roskilde, Denmark; praveen@ruc.dk

² Center for Virtual Learning Technologies, Roskilde University, 4000 Roskilde, Denmark

³ Climate Change Research Division, Korea Institute of Energy Research, Daejeon 34129, Korea; jiye.lee@kier.re.kr (J.L.); vijayan.mibi@gmail.com (D.V.); syl@kier.re.kr (S.Y.L.)

⁴ Graduate School of Energy Science and Technology, Chungnam National University, Daejeon 34134, Korea; kyubock.lee@cnu.ac.kr

⁵ Department of Chemical & Biological Engineering, Korea University, Seoul 02841, Korea; simsj@korea.ac.kr (S.J.S.); finalarea@naver.com (M.E.H.)

⁶ School of Chemical & Biomolecular Engineering, Pusan National University, Busan 46241, Korea; alflso0191@pusan.ac.kr

* Correspondence: youkwan@pusan.ac.kr; Tel.: +82-51-510-2395

Received: 12 December 2019; Accepted: 6 January 2020; Published: 10 January 2020



Abstract: *Haematococcus pluvialis* accumulates astaxanthin, which is a high-value antioxidant, during the red cyst stage of its lifecycle. The development of a rigid cell wall in the cysts hinders the recovery of astaxanthin. We investigated morphological changes and cell disruption of mature *H. pluvialis* cyst cells while using high-pressure homogenization for astaxanthin extraction. When treated with French-press-cell (pressure, 10,000–30,000 psi; passage, 1–3), the intact cyst cells were significantly broken or fully ruptured, releasing cytoplasmic components, thereby facilitating the separation of astaxanthin by ethyl acetate. Fluorescence microscopy observations using three different fluorescent dyes revealed that a greater degree of cell breakage caused greater external dispersion of astaxanthin, chlorophyll, lipids, proteins, and carbohydrates. The mechanical treatment resulted in a high cell disruption rate of up to 91% based on microscopic cell typing and Coulter methods. After the ethyl acetate extraction, the astaxanthin concentration significantly increased by 15.2 mg/L in proportion to the increase in cell disruption rate, which indicates that cell disruption is a critical factor for solvent-based astaxanthin recovery. Furthermore, this study recommends a synergistic combination of the fast instrumental particle-volume-distribution analysis and microscope-based morphologic phenotyping for the development of practical *H. pluvialis* biorefinery processes that co-produce various biological products, including lipids, proteins, carbohydrates, chlorophyll, and astaxanthin.

Keywords: *Haematococcus pluvialis*; high-pressure homogenization; astaxanthin; cyst; cell disruption

1. Introduction

Microalgal biomass is currently considered as a promising resource for valuable biochemicals and biofuels [1,2]. Especially, astaxanthin (3,3'-dihydroxy- β -carotene-4,4'-dione), which is a secondary ketocarotenoid compound, has been widely applied in feed, cosmetic, and pharmaceutical industries, owing to its excellent antioxidant, anti-inflammatory, and anti-cancer properties [3–5]. Although synthetic astaxanthin is extensively used as feed additives in aquaculture, natural astaxanthin is preferred over synthetic form for human consumption in view of its mixture of isomers and safety

concerns [6,7]. Several commercial-scale facilities currently produce natural astaxanthin from green microalga *Haematococcus pluvialis* having high astaxanthin content (~4%, w/w) [8,9].

H. pluvialis cell wall is difficult to destroy due to the considerable thickness and rigidity that are associated with its multiple layers formed during the transformation from green vegetative cells to astaxanthin-rich red cysts [10,11]. Apart from astaxanthin recovery, a biorefinery process that can co-produce other cellular components, such as lipids, proteins, and carbohydrates, can significantly reduce the cost of large-scale *H. pluvialis*-based astaxanthin production [12,13]. Accordingly, efforts to develop an environmental-friendly and cost-effective cell disruption process from *H. pluvialis* is practically in progress. Various chemical and supercritical fluid extractions of astaxanthin from *H. pluvialis* biomass have been extensively studied [14,15]. However, the chemical treatment is potentially harmful with the excessive use of strong organic solvent (s) resulting in a lower stability and quality of astaxanthin [8]. The supercritical CO₂ extraction process requires longer operation time and, generally, the use of co-solvent(s) and/or physicochemical pretreatment. Furthermore, this method is very expensive for large-scale biorefining applications [8,14].

High-pressure homogenization has been proposed as a relatively simple and importantly scalable cell disruption method for industrial-scale microalgal biorefining processes among various mechanical techniques, including bead milling, high-pressure homogenization, ultrafine grinding, autoclave, and sonication [8,12]. However, although there have been several studies on oleaginous *Chlorella* and *Nannochloropsis* species, especially for biodiesel production, application on harder aplanospore-forming species (e.g., *H. pluvialis*) is relatively limited [16].

In this study, the efficiency of astaxanthin recovery according to cellular disruption level of *H. pluvialis* cyst cells was investigated by controlling high pressures (10,000–30,000 psi) and passages (1–3) of a French press cell as a model high-pressure homogenization method. During the mechanical cell disruption, the cell types were classified as intact, leaky, and ruptured based on optical microscopy. The size distribution of cellular particles and spatial distribution of intracellular biomolecules (e.g., astaxanthin, lipids, proteins, carbohydrates, and chlorophyll) were also characterized while using a Coulter counter and staining-based fluorescence microscopy techniques, respectively. Specific insights on their morphological changes and distributions will be beneficial for efficient scale-up and biorefinery applications. Finally, the technical feasibility of a fast instrumental Coulter counter was investigated as an alternative to the conventional time-consuming microscopic cell classification as an indicator of the algal cell disruption level [17].

2. Materials and Methods

2.1. Materials

Professor Sang Jun Sim of Korea University, Seoul, Korea provided the intact cysts of *H. pluvialis* NIES-144 that were used in this study. NIES-144 strain was originally obtained from the National Institute for Environmental Studies (NIES), Tsukuba, Japan, and cultivated in thin-film photobioreactors (working volume, ~63 L) under outdoor photoautotrophic conditions while using a CO₂-rich (~3.5%, v/v) power-plant flue gas (Korean District Heating Co., Pangyo, Gyeonggi, Korea). Comprehensive medium composition and culture conditions are available in the literature [18]. The *H. pluvialis* cysts were harvested by centrifugation (1100× *g*, 10 min., 4 °C; Supra 22K, Hanil Science Inc., Gimpo, Korea), washed three times with purified water (Millipore Milli-Q system, Japan), and then freeze-dried for 48 h (FD5512, IIShin BioBase Co., Gyeonggi, Korea). The lyophilized *H. pluvialis* biomass was preserved in a sterile vacuum bag and stored at −20 °C in a dark environment until further use.

All of the organic solvents and chemicals used in this study were of analytical grade and from Junsei (Tokyo, Japan) and Sigma Aldrich (St. Louis, MO, USA). Astaxanthin standard was purchased from Dr. Ehrenstorfer GmbH (Augsburg, Germany). The fatty acid methyl ester (FAME) (Mix RM3, Mix RM5, GLC50, and GLC70) and sugar (D-glucose, D-arabinose, D-mannose, D-galactose, and D-xylose) standards were supplied from Sigma Aldrich (St. Louis, MO, USA).

2.2. Mechanical Cell Disruption

High-pressure homogenization method (French press cell, Thermo Electron Co., Waltham, MA, USA) was applied to algal biomass in three passes at three different pressures (10,000, 20,000, and 30,000 psi) to disrupt *H. pluvialis* cysts. The freeze-dried *H. pluvialis* biomass was dispersed in distilled water (Millipore Milli-Q system, Tokyo, Japan) at 1.0 g/L and vigorously mixed in a vortex (Vortex 3, IKA, Staufen, Germany) to ensure the homogeneity of the algal sample. The maximum internal capacity of the French press cell was 30 mL and the working volume in this study was fixed at 20 mL. In this process, the algal cells (1.0 g/L) are forced to flow through a very small orifice under high-pressure conditions, and, as a result, they could be disrupted by synergistic mechanical effects, such as cavitation, turbulence, and shear stress [12].

2.3. Microscopic Observation

The cell disruption and distribution of internal biomolecules of *H. pluvialis* cyst cells were observed under a bright field and fluorescence microscope (Carl Zeiss imager A2, Oberkochen, Germany). In the bright field mode, after the high-pressure homogenization, *H. pluvialis* cysts containing astaxanthin (red color) could be largely classified into intact, leaky, and ruptured types while considering their morphological changes due to mechanical breakages.

Cell staining was carried out in the order of proteins, carbohydrates, and lipids in order to simultaneously visualize the cell wall and various cytoplasmic components. To stain proteins, 100 μ L of sodium carbonate buffer (0.1 M) and 10 μ L of fluorescein isothiocyanate solution (FITC, 10 mg/mL) were added into the algal sample. Afterwards, the solution was stirred for 1 h at room temperature. Next, for carbohydrate staining, the cells were washed twice with phosphate buffer saline (pH = 7.2), and 100 μ L of Calcofluor white reagent (300 mg/L) was added thereto and then incubated for 30 min. Again, washing was performed twice with phosphate buffer saline (pH = 7.2), followed by the addition of 10 μ L of Nile red solution (20 mg/mL) for neutral lipid detection. Following this, the sample was incubated in a dark environment for 10 min. and then washed twice with phosphate buffer saline (pH = 7.2). In the fluorescent mode, the blue color of the carbohydrates was observed while using filter set 49, the green color of proteins and red color of chlorophyll auto-fluorescence was observed using filter set A9, and the yellow color of neutral lipids was observed using filter set 09.

2.4. Cell Disruption Efficiency Estimation

Instrumental particle-counting and microscopic cell typing methods evaluated cell disruption efficacy during the high-pressure homogenization. A Coulter counter (MultisizerTM 4, Beckman Coulter, Brea, CA, USA) with a 100 μ m aperture tube was used for determining the bio-volume, size, and number of particles in the range of 2–60 μ m. The sample volume was adjusted to 100 mL while using Isoton II electrolyte solution (Beckman Coulter, Brea, CA, USA) in the way that the particle concentration was kept below 10%. The cell disruption efficiency (%) was estimated from the total bio-volume reduction degree of the homogenized sample versus the untreated control (100%). The total volume of particles was calculated by summing each volume of all the particles in the selected size range (especially 15–60 μ m). The cell disruption degree (i.e., the remaining intact type no/total cell no. after the mechanical treatment) was also estimated by manually sorting over 100 cells while using an improved Neubauer counting chamber (C-Chip, DHC-N01, iNCYTO, Chungnam, Korea) based on the optical microscope mentioned above.

2.5. Other Analytical Methods

For astaxanthin extraction, 1 mL of French-press-treated *H. pluvialis* cells was vigorously mixed in a vortex mixer (Vortex 3, IKA, Germany) with 5 mL of ethyl acetate for 10 min. at room temperature. The mixture was separated by centrifugation (2000 \times g, 10 min.; Combi-514R, Hanil Science Inc., Gimpo, Korea) and an astaxanthin-containing organic fraction was collected and evaporated (N-EVAP

evaporator; Organomation Associates Inc., Berlin, MA, USA). After saponification reaction with 0.025 N NaOH, free (de-esterified) astaxanthin content was analyzed while using a high-performance liquid chromatography (HPLC, Agilent 1260 series, Agilent, Santa Clara, CA, USA) that was equipped with a variable wavelength detector (VWD) and 250 × 4.6 mm YMC carotenoid column (Tokyo, Japan). The detailed extraction and HPLC conditions are detailed in the literature [6,19].

Lipid content of the freeze-dried *H. pluvialis* cysts was estimated by the FAME amount, according to a direct transesterification method, followed by gas chromatography (GC) [6,19]. Briefly, for lipid extraction, 2 mL of the chloroform/methanol (2:1, v/v) was added to the algal cells (~10 mg in a 12 mL Pyrex-glass tube). For the FAME analysis, subsequently, 1 mL of chloroform containing heptadecanoic acid (C17:0) as an internal standard (500 µg/L), 1 mL of methanol, and 300 µL of H₂SO₄ (95%) were added to the glass tube. The tube was incubated at 100 °C for 10 min. (HS R200 heating-block reactor, Humas, Daejeon, Korea), cooled to room temperature, and then supplemented with 1 mL of distilled water. Finally, the FAME-containing organic phase was filtered by a PVDF (polyvinyl difluoride) syringe filter and then analyzed by GC that was equipped with a flame-ionization detector and a 0.32 mm (ID) × 30 m HP-INNOWax capillary column (Agilent Technologies, Santa Clara, California, USA). The detailed GC conditions are available in [19].

Carbohydrate amount was estimated according to the NREL/TP-510-42618 protocol [20]. For cell hydrolysis, approximately 300 mg of the lyophilized *H. pluvialis* cells was mixed with 3 mL of H₂SO₄ solution (72%) in a Pyrex-glass tube and then incubated for 60 min. at 30 °C. Subsequently, 84 mL of purified water (Millipore Milli-Q system, Tokyo, Japan) was added and further incubated for 1 h at 121 °C while using an autoclave (Napco 8000-DSE, Thermo Scientific Co., Waltham, MA, USA). The carbohydrate extract was cooled down to room temperature, centrifuged at 15,000× g for 5 min. (Combi-514R, Hanil Science Inc., Korea), and then PVDF syringe-filtered. Finally, the filtrate was analyzed using a HPLC equipped with a refractive-index (RI) detector (Agilent 1260, Agilent Co., Santa Clara, CA, USA) and Aminex HPX-87H column (300 × 7.8 mm, Bio-Rad, Hercules, CA, USA). As an eluent, 5 mM H₂SO₄ solution was used at a flow rate of 0.5 mL/min. The temperatures of column and RI detector were set at 60 °C and 50 °C, respectively.

3. Results and Discussion

3.1. Morphological Changes by Mechanical Disruption

The effect of French press cell treatment (10,000 psi, 1 pass) on mature *H. pluvialis* cysts were evaluated morpho-dynamically while using a combination of light and fluorescence microscopy (Figure 1). In the phase-contrast mode of optical microscope, the intact *H. pluvialis* cysts showed significant amounts of astaxanthin (bright red) and chlorophyll (green) inside the cells. The high-pressure homogenization could partially damage or completely rupture the cell walls of the cysts, resulting in significant releases of the cytoplasmic constituents into the surrounding medium. The *H. pluvialis* cysts could be largely categorized into intact, leaky, and ruptured types, depending on their degree of destruction (see Figure 2 for their distribution).

Three different fluorescent probes of Calcofluor white, Nile red, and FITC were used under fluorescence microscopy, respectively, in order to simultaneously visualize the cell wall and cytoplasmic polysaccharides (blue), neutral lipids (yellow), and proteins (green) of *H. pluvialis* cyst cells. Figure 1 shows astaxanthin (magenta) and chlorophyll (red) auto-fluoresce without chemical staining. The total carbohydrate content of the *H. pluvialis* cysts that were incubated under the outdoor conditions while using a CO₂-rich (~3.5%, v/v) power-plant flue gas was estimated to be 12% (w/w). With the Calcofluor white dye, the polysaccharide fractions of the cell wall and the cytoplasmic contents were stained blue under the DAPI filter. The intact encysted cells showed a continuous blue color on their cell walls, because the *H. pluvialis* cell wall is mostly composed of mannan and cellulose polysaccharides [21,22]. However, significant dispersion of the blue-colored cell wall and cytoplasmic polysaccharides were observed after mechanical disruption.

Nile-red-stained neutral lipids are usually detected as cytoplasmic yellow-colored droplets in oleaginous microalgal species, such as *Chlorella* [23] and *Nannochloropsis* [24], under fluorescent microscopy. The total lipid content of the *H. pluvialis* cyst cell was as high as 40% (w/w) when estimated in terms of FAME amount by GC. This is similar to the typical lipid compositions of *H. pluvialis* (32–37% (w/w)) harvested from the red cultivation stage [25]. However, it should be noted that, in *H. pluvialis* cysts, astaxanthin biomolecules co-exist inside the lipid body mostly in mono- and di-ester forms with long-chain fatty acids [26,27]. Therefore, under the present fluorescence microscopy condition, the former (magenta) and latter (yellow) cannot be clearly distinguished from the intact and leaky cell types. However, interestingly, after almost the complete rupture of the *H. pluvialis* cyst cells, several yellow-colored lipid droplets appeared from the dispersed cytoplasm. The protein fractions from *H. pluvialis* cells fluoresced green after the FITC staining. As expected, the intact cysts showed a relatively uniform green distribution in the cytosol, except for lipids, astaxanthin, and chlorophyll. However, following the mechanical treatment, the intensity of green color was significantly reduced. This might be mainly attributed to the significant loss of water-soluble proteins in the medium. Overall, the degree of dispersion of the internal constituents, including astaxanthin, increased in proportion to the degree of cell rupture. This resulted in the effective recovery of astaxanthin from the robust *H. pluvialis* cysts by subsequent solvent extraction (see next sections).

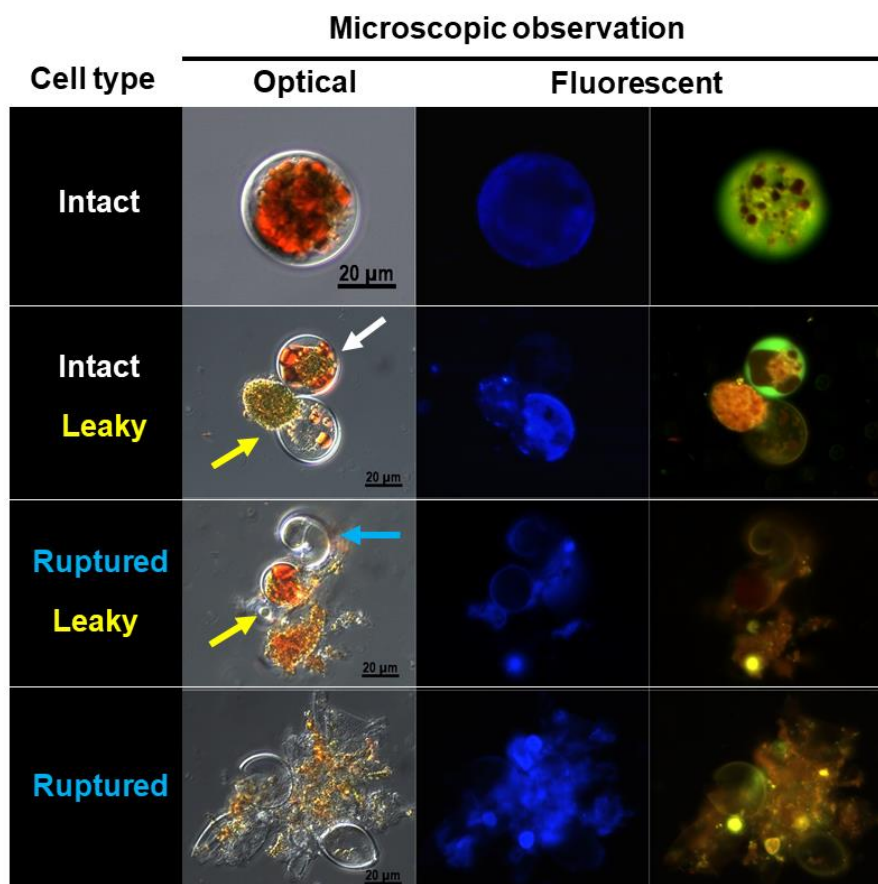


Figure 1. Microscopic images of *H. pluvialis* cysts after the high-pressure homogenization treatment (10,000 psi and one pass). Cell shapes were classified into three types (i.e., intact, leaky, and ruptured) considering their morphological changes by the mechanical breakages. See colored arrows for each cell type. From left to right, optical phase-contrast images; fluorescent images under DAPI filter showing the cell wall and other polysaccharides (blue stained with Calcofluor white); fluorescent images under fluorescein isothiocyanate solution (FITC) long-pass filter showing the proteins (green stained with FITC), lipids (yellow stained with Nile red), chlorophyll (red by auto-fluorescence), and astaxanthin (magenta by auto-fluorescence).

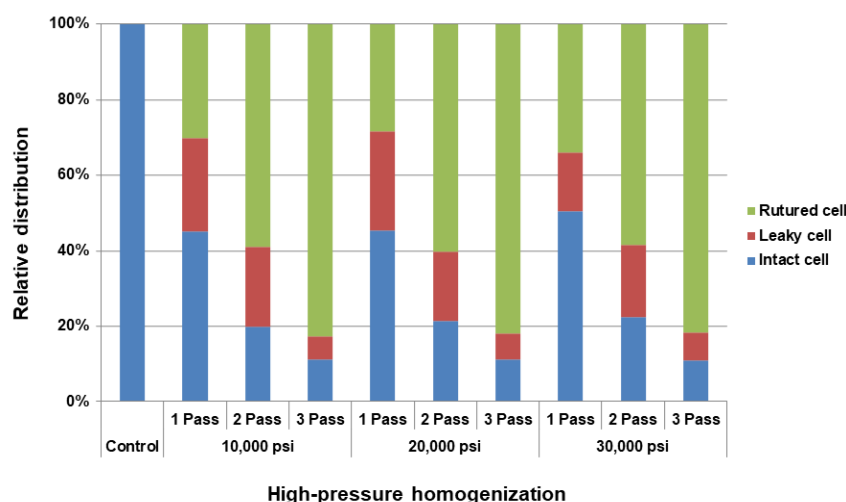


Figure 2. Cell type distribution of *H. pluvialis* cysts after various high-pressure homogenization treatments (pressure, 10,000–30,000 psi; passage, 1–3). The cell types were classified into intact, leaky, and ruptured according to the morphological features that are based on the microscopic observation (Figure 1).

3.2. Cell Type Distribution by Microscopic Counting

Figure 2 shows the relative cell type distribution of *H. pluvialis* cysts after various high-pressure homogenization treatments (pressure intensity, 10,000–30,000 psi; pass, 1–3 times). The morphological cell types were calculated by sorting over 100 cells while using the improved Neubauer counting chamber under microscopic observation (also see Figure 1). After the homogenization in one pass at a pressure of 10,000 psi, the number of intact cyst cells accounted for ca. 45%, whereas the rest of the initial cysts became either leaky or ruptured completely (cell disruption, $54.8 \pm 0.3\%$). Here, the cell disruption (%) was estimated by subtracting the % ratio of both the leaky and ruptured cells from the initial cells (100%). The cell disruption degree significantly increased to $80.2 \pm 6.0\%$ and $89 \pm 0.8\%$, respectively, when the algal-suspension was homogenized once and twice more at the same pressure. On the contrary, at higher pressures of 20,000–30,000 psi, the cell disruption efficiency of *H. pluvialis* cysts did not improve when compared to that of the 10,000 psi treatment even if the passage number was increased from 1 to 3. The cell disruption efficacy of the high-pressure homogenization process can be influenced by the algal cell concentration, as well as the homogenizer specification (loading pressure and number of passage) [12]. Lowering the cell dosage might be considered in order to improve the cell disruption rate to more than 90%. However, it should be noted that this approach is not generally recommended in terms of large-scale biorefining of *H. pluvialis* biomass on an industrial scale [8].

Although the high-pressure homogenization has been recommended as a relatively efficient and scalable method among various physicochemical cell disruption techniques for large-scale algal biorefining [8,12], studies on *H. pluvialis* cyst cells are very limited. Praveenkumar et al. [19] reported that, when compared to ionic liquid-based extractions, the 30,000 psi-fixed high-pressure homogenization resulted in a high yield of 24 pg astaxanthin/cell from wet *H. pluvialis* cysts that were cultured under small-scale laboratory conditions. However, the cell disruption rate and key operating parameters (especially pressure intensity and number of passages) were not elucidated. Safi et al. [17] obtained the highest protein extraction yield (40%) from lyophilized *H. pluvialis* biomass while using a high-pressure cell disruptor that was fixed at 2700 bar (39,150 psi), as compared to manual grinding, alkaline treatment, and ultrasonication treatments. Moreover, they reported that, under the same condition, the maximal protein recovery efficiency showed a decreasing trend in accordance with the increasing order of cell wall rigidity among the tested algal strains: *Arthrospira platensis* < *Porphyridium cruentum* < *Chlorella vulgaris* < *Nannochloropsis oculata* < *H. pluvialis*. Detailed investigation into cell physiology, cell wall biology, and physical strength of *H. pluvialis* cells is required in order to develop an

economical high-pressure homogenization process. In fact, this insight would create high potentialities for a synergistic or novel process that utilizes various existing biological–physicochemical treatments.

3.3. Bio-Particle Distribution by Coulter Counter and Astaxanthin Recovery

Figure 3 shows the bio-volume distribution and total bio-volume of *H. pluvialis* bio-particles before and after French press cell treatment with different pressures (10,000–30,000 psi) and then passes (1–3). Here, “bio-particles” collectively refer to the ruptured cells, cell debris, and internal biomolecules that have leaked outwards, as well as the initial intact cells. In the untreated control, most of the *H. pluvialis* cysts were of 15–60 μm cell size and they exhibited a relatively large particle volume distribution ($\sim 4.1 \times 10^7 \mu\text{m}^3/\text{mL}$) (Figure 3a). However, when homogenized at a pressure of 10,000 psi, the particle volumes of bio-particles in the same range significantly decreased in proportion to the increase in the number of passage: $\sim 1.7 \times 10^7 \mu\text{m}^3/\text{mL}$ for one pass, $\sim 1.3 \times 10^7 \mu\text{m}^3/\text{mL}$ for two passes, and $\sim 0.5 \times 10^7 \mu\text{m}^3/\text{mL}$ for three passes. On the contrary, the volumes of the bio-particles smaller than $\sim 15 \mu\text{m}$ increased slightly when compared to the untreated control. These changes were induced by the mechanical destruction of the initial cyst cells (see Figure 1 for morphological changes).

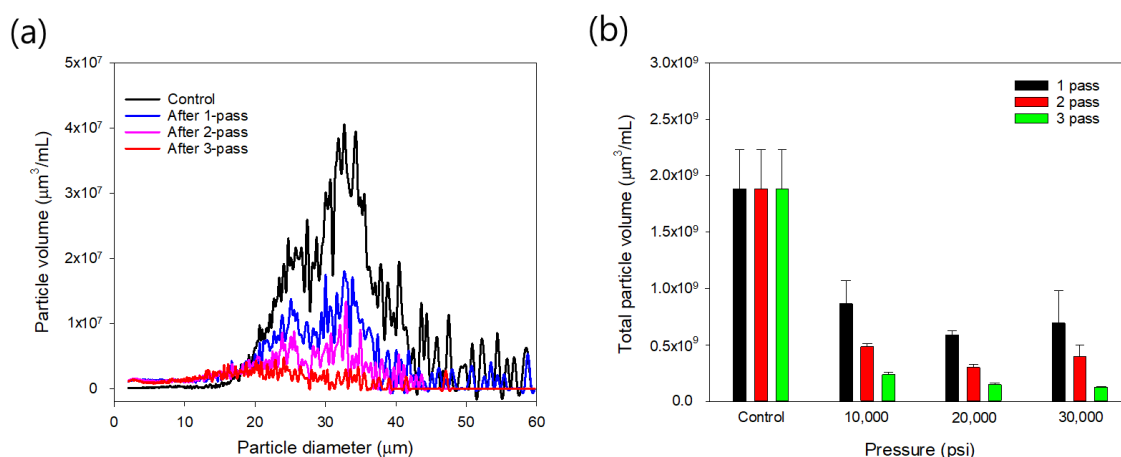


Figure 3. Changes in volume distribution (a) and total volume (b) of *H. pluvialis* bio-particles after mechanical disruptions with different pressures and passes. The bio-particles refer to all internal components as well as intact, leaky, and ruptured cyst cells. Representative particle-size-volume distributions after the 10,000 psi-homogenizations at three different passes were presented based on the Coulter counter analysis. Total volumes were calculated by summing each volume of all particles sized between 15 and 60 μm .

Figure 3b plotted the changes in the total bio-volumes of the bio-particles after the homogenization treatments. The total bio-volume of the homogenized bio-particles was calculated by summing the volume of each bio-particle between 15 to 60 μm while considering their characteristic volume reductions. The total bio-volume of the untreated *H. pluvialis* cysts ($1.9 \times 10^9 \mu\text{m}^3/\text{mL}$) decreased almost linearly with an increasing number of passes (1–3), irrespective of the tested pressure intensity (10,000–30,000 psi). However, no significant positive effect of the high pressures (20,000–30,000 psi) was observed as compared to the case of 10,000 psi, which is similar to that of the microscopic cell typing (Figure 2). The cell disruption efficiency could be simply derived from the degree of total volume reduction of the homogenized samples (versus the untreated control, 100%), and its maximal value was estimated to be $91.8 \pm 2.2\%$. This value was also almost equal to the highest value ($89 \pm 0.8\%$) that was obtained from the microscopic cell counting in Figure 2.

When comparing the cell disruption efficiencies that were calculated from Coulter counting and microscopic cell typing methods, a statistically good correlation ($r^2 = 0.95$) was obtained (Figure 4a). Furthermore, by the subsequent ethyl acetate extraction, astaxanthin was recovered from the *H. pluvialis* biomass treated under various high-pressure homogenization conditions (see Figures 2 and 3). As

expected, the astaxanthin concentration increased almost linearly from 5.3 to 15.2 mg/L in proportion to the increase in cell disruption level (Figure 4b), which indicated that cell disruption is a critical factor for solvent-based astaxanthin recovery. The astaxanthin content of the *H. pluvialis* biomass was estimated to be 1.1% (w/w). Astaxanthin from the freeze-dried *H. pluvialis* cyst cells could also be extracted while using solely ethyl acetate, although its concentration was as low as 5.3 mg/L. The statistical r^2 values for relationships between the astaxanthin recovery and cell disruption degree were estimated to be 0.83 and 0.86 for the microscopic and Coulter counter methods, respectively. This result suggests that the Coulter counter method can be used effectively for the rapid assessment of *H. pluvialis* cell disruption for astaxanthin recovery. Microscopy phenotyping generally requires time-consuming and laborious experimentation by skilled personnel. However, it should be noted that this approach is very useful in understanding the actual morphological changes of the rigid *H. pluvialis* cysts and the spatial distribution of the target biomolecules during mechanical treatment (Figure 1). Therefore, a synergistic combination of these methods is recommended for the development of practical *H. pluvialis* biorefinery processes that co-produce various bio-products, including lipids, proteins, carbohydrates, chlorophyll, and astaxanthin. Several analytical techniques have been reported in order to evaluate the disintegration efficiency of algal biomass by mechanical treatments: particle-size analyzer (homogenization for *Chlamydomonas reinhardtii* and *Pseudokirchneriella subcapitata* [28]; bead beating for *C. reinhardtii* [29]), dynamic light scattering (ultrasonication for *Parachlorella kessleri* [30]), and flow cytometer (bead milling for *Chlorella* species [31,32]). However, after cell disruption, the morphological characteristics of the algal cell and/or the internal target substance(s) have not been studied in detail.

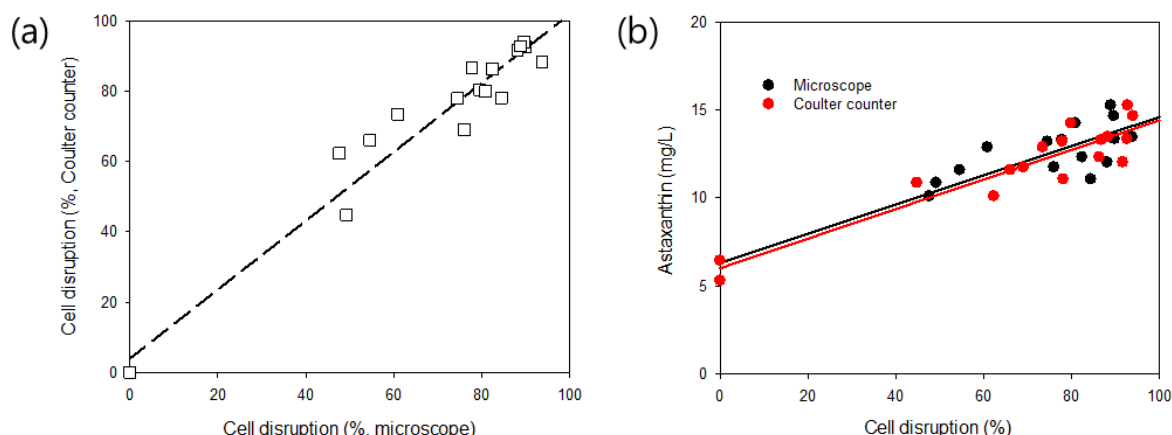


Figure 4. (a) Cell disruption efficiency relationship between microscopic cell typing and instrumental particle-size-distribution measurements ($r^2 = 0.95$); (b) astaxanthin recovery, depending on cell disruption efficiencies (microscope, $r^2 = 0.83$; Coulter counter, $r^2 = 0.86$).

4. Conclusions

High-pressure homogenization might be used for highly efficient cell disruption and astaxanthin recovery from mature *H. pluvialis* cyst cells, followed by ethyl acetate extraction. French press cell treatment effectively destroys the *H. pluvialis* cyst cells and results in a high disruption rate of up to 91%. The homogenized cells can be classified into intact, leaky, and completely ruptured, according to their morphological changes under an optical microscope. The degree of external dispersion of astaxanthin, lipids, proteins, and carbohydrates was almost proportional to the degree of cell rupture when analyzed by fluorescence microscopy with specific fluorescent probes. Pressure intensity (10,000–30,000 psi) did not affect the cell disruption efficiency, but an increasing the number of passages (1–3 times) could significantly improve the cell disruption efficiency. After the subsequent ethyl acetate extractions, the astaxanthin concentration increased linearly from 5.3 to 15.2 mg/L with increased cell disruption

efficacy owing to homogenization optimization. The maximum astaxanthin recovery was estimated to be 1.1% (weight of dry cells).

Author Contributions: Conceptualization, R.P. and K.L.; methodology, R.P., J.L., D.V., M.E.H. and S.J.S.; Writing—Original draft preparation, R.P.; Writing—Review and editing, R.P., Y.-K.O., Y.-E.K. and S.Y.L.; supervision, Y.-K.O.; funding acquisition, Y.-K.O. All authors have read and agreed to the published version of the manuscript.

Funding: This work was supported by the National Research Foundation of Korea (grant number: NRF-2019R1A2C1003463) funded by the Ministry of Science and ICT and the Research/Development Program of the Korea Institute of Energy Research (grant number: KIER-B9-2442-04). Sim, S.J., also would like to acknowledge the support of the Korea CCS R & D Center (Korea CCS 2020 Project) funded by the Ministry of Science and ICT in 2017 (grant number: KCRC-2014M1A8A1049278).

Conflicts of Interest: The authors declare no conflict of interest.

References

1. Bauer, A.; Minceva, M. Direct extraction of astaxanthin from the microalgae: *Haematococcus pluvialis* using liquid-liquid chromatography. *RSC Adv.* **2019**, *9*, 22779–22789. [\[CrossRef\]](#)
2. Matter, I.A.; Hoang Bui, V.K.; Jung, M.; Seo, J.Y.; Kim, Y.E.; Lee, Y.C.; Oh, Y.K. Flocculation harvesting techniques for microalgae: A review. *Appl. Sci.* **2019**, *9*, 3069. [\[CrossRef\]](#)
3. Focsan, A.L.; Polyakov, N.E.; Kispert, L.D. Photo protection of *Haematococcus pluvialis* algae by astaxanthin: Unique properties of astaxanthin deduced by EPR, optical and electrochemical studies. *Antioxidants* **2017**, *6*, 80. [\[CrossRef\]](#) [\[PubMed\]](#)
4. Guerin, M.; Huntley, M.E.; Olaizola, M. *Haematococcus* astaxanthin: Applications for human health and nutrition. *Trends Biotechnol.* **2003**, *21*, 210–216. [\[CrossRef\]](#)
5. Pérez-López, P.; González-García, S.; Jeffries, C.; Agathos, S.N.; McHugh, E.; Walsh, D.; Murray, P.; Moane, S.; Feijoo, G.; Moreira, M.T. Life cycle assessment of the production of the red antioxidant carotenoid astaxanthin by microalgae: From lab to pilot scale. *J. Clean. Prod.* **2014**, *64*, 332–344. [\[CrossRef\]](#)
6. Choi, S.A.; Oh, Y.K.; Lee, J.; Sim, S.J.; Hong, M.E.; Park, J.Y.; Kim, M.S.; Kim, S.W.; Lee, J.S. High-efficiency cell disruption and astaxanthin recovery from *Haematococcus pluvialis* cyst cells using room-temperature imidazolium-based ionic liquid/water mixtures. *Bioresour. Technol.* **2019**, *274*, 120–126. [\[CrossRef\]](#) [\[PubMed\]](#)
7. Samori, C.; Pezzolesi, L.; Galletti, P.; Semeraro, M.; Tagliavini, E. Extraction and milking of astaxanthin from: *Haematococcus pluvialis* cultures. *Green Chem.* **2019**, *21*, 3621–3628. [\[CrossRef\]](#)
8. Kim, D.Y.; Vijayan, D.; Praveenkumar, R.; Han, J.I.; Lee, K.; Park, J.Y.; Chang, W.S.; Lee, J.S.; Oh, Y.K. Cell-wall disruption and lipid/astaxanthin extraction from microalgae: *Chlorella* and *Haematococcus*. *Bioresour. Technol.* **2016**, *199*, 300–310. [\[CrossRef\]](#)
9. Panis, G.; Carreon, J.R. Commercial astaxanthin production derived by green alga *Haematococcus pluvialis*: A microalgae process model and a techno-economic assessment all through production line. *Algal Res.* **2016**, *18*, 175–190. [\[CrossRef\]](#)
10. Cheng, X.; Riordon, J.; Nguyen, B.; Ooms, M.D.; Sinton, D. Hydrothermal disruption of algae cells for astaxanthin extraction. *Green Chem.* **2017**, *19*, 106–111. [\[CrossRef\]](#)
11. Machado, F.R.S.; Trevisol, T.C.; Boschetto, D.L.; Burkert, J.F.M.; Ferreira, S.R.S.; Oliveira, J.V.; Burkert, C.A.V. Technological process for cell disruption, extraction and encapsulation of astaxanthin from *Haematococcus pluvialis*. *J. Biotechnol.* **2016**, *218*, 108–114. [\[CrossRef\]](#) [\[PubMed\]](#)
12. Lee, S.Y.; Cho, J.M.; Chang, Y.K.; Oh, Y.K. Cell disruption and lipid extraction for microalgal biorefineries: A review. *Bioresour. Technol.* **2017**, *244*, 1317–1328. [\[CrossRef\]](#) [\[PubMed\]](#)
13. Khoo, K.S.; Lee, S.Y.; Ooi, C.W.; Fu, X.; Miao, X.; Ling, T.C.; Show, P.L. Recent advances in biorefinery of astaxanthin from *Haematococcus pluvialis*. *Bioresour. Technol.* **2019**, 121606. [\[CrossRef\]](#) [\[PubMed\]](#)
14. Reyes, F.A.; Mendiola, J.A.; Ibañez, E.; Del Valle, J.M. Astaxanthin extraction from *Haematococcus pluvialis* using CO₂-expanded ethanol. *J. Supercrit. Fluids* **2014**, *92*, 75–83. [\[CrossRef\]](#)
15. Sarada, R.; Vidhyavathi, R.; Usha, D.; Ravishankar, G.A. An efficient method for extraction of astaxanthin from green alga *Haematococcus pluvialis*. *J. Agric. Food Chem.* **2006**, *54*, 7585–7588. [\[CrossRef\]](#)
16. Park, J.Y.; Oh, Y.K.; Choi, S.A.; Kim, M.C. Recovery of astaxanthin-containing oil from *Haematococcus pluvialis* by nano-dispersion and oil partitioning. *Appl. Biochem. Biotechnol.* **2020**, 1–15. [\[CrossRef\]](#)

17. Safi, C.; Ursu, A.V.; Laroche, C.; Zebib, B.; Merah, O.; Pontalier, P.Y.; Vaca-Garcia, C. Aqueous extraction of proteins from microalgae: Effect of different cell disruption methods. *Algal Res.* **2014**, *3*, 61–65. [\[CrossRef\]](#)
18. Choi, Y.Y.; Hong, M.E.; Jin, E.S.; Woo, H.M.; Sim, S.J. Improvement in modular scalability of polymeric thin-film photobioreactor for autotrophic culturing of *Haematococcus pluvialis* using industrial flue gas. *Bioresour. Technol.* **2018**, *249*, 519–526. [\[CrossRef\]](#)
19. Praveenkumar, R.; Lee, K.; Lee, J.; Oh, Y.K. Breaking dormancy: An energy-efficient means of recovering astaxanthin from microalgae. *Green Chem.* **2015**, *17*, 1226–1234. [\[CrossRef\]](#)
20. Sluiter, A.; Hames, B.; Ruiz, R.; Scarlata, C.; Sluiter, J.; Templeton, D.; Crocker, D. NREL/TP-510-42618 analytical procedure—Determination of structural carbohydrates and lignin in biomass. *Lab. Anal. Proced.* **2008**, *1617*, 1–16.
21. Hagen, C.; Siegmund, S.; Braune, W.; Botanik, A.; Jena, F.; Planetarium, A. Ultrastructural and chemical changes in the cell wall of *Haematococcus pluvialis* (Volvocales, Chlorophyta) during aplanospore formation. *Eur. J. Phycol.* **2002**, *37*, 217–226. [\[CrossRef\]](#)
22. Damiani, M.C.; Leonardi, P.I.; Pieroni, O.I.; Cáceres, E.J. Ultrastructure of the cyst wall of *Haematococcus pluvialis* (Chlorophyceae): Wall development and behaviour during cyst germination. *Phycologia* **2006**, *45*, 616–623. [\[CrossRef\]](#)
23. Lee, Y.C.; Lee, H.U.; Lee, K.; Kim, B.; Lee, S.Y.; Choi, M.H.; Farooq, W.; Choi, J.S.; Park, J.Y.; Lee, J.; et al. Aminoclay-conjugated TiO₂ synthesis for simultaneous harvesting and wet-disruption of oleaginous *Chlorella* sp. *Chem. Eng. J.* **2014**, *245*, 143–149. [\[CrossRef\]](#)
24. Wei, L.; Huang, X. Long-duration effect of multi-factor stresses on the cellular biochemistry, oil-yielding performance and morphology of *Nannochloropsis oculata*. *PLoS ONE* **2017**, *12*, e0174646. [\[CrossRef\]](#) [\[PubMed\]](#)
25. Shah, M.M.R.; Liang, Y.; Cheng, J.J.; Daroch, M. Astaxanthin-producing green microalga *Haematococcus pluvialis*: From single cell to high value commercial products. *Front. Plant Sci.* **2016**, *7*, 531. [\[CrossRef\]](#)
26. Ding, W.; Li, Q.; Han, B.; Zhao, Y.; Geng, S.; Ning, D. Comparative physiological and metabolomic analyses of the hyper-accumulation of astaxanthin and lipids in *Haematococcus pluvialis* upon treatment with butylated hydroxyanisole. *Bioresour. Technol.* **2019**, *292*, 122002. [\[CrossRef\]](#) [\[PubMed\]](#)
27. Peled, E.; Leu, S.; Zarka, A.; Weiss, M.; Pick, U.; Khozin-Goldberg, I.; Boussiba, S. Isolation of a novel oil globule protein from the green alga *Haematococcus pluvialis* (chlorophyceae). *Lipids* **2011**, *46*, 851–861. [\[CrossRef\]](#)
28. Lavoie, M.; Bernier, J.; Fortin, C.; Campbell, P.G.C. Cell homogenization and subcellular fractionation in two phytoplanktonic algae: Implications for the assessment of metal subcellular distributions. *Limnol. Oceanogr. Methods* **2009**, *7*, 277–286. [\[CrossRef\]](#)
29. Lam, G.P.; Van Der Kolk, J.A.; Chordia, A.; Vermuë, M.H.; Olivieri, G.; Eppink, M.H.M.; Wijffels, R.H. Mild and selective protein release of cell wall deficient microalgae with pulsed electric field. *ACS Sustain. Chem. Eng.* **2017**, *5*, 6046–6053. [\[CrossRef\]](#)
30. Piasecka, A.; Cieřła, J.; Koczańska, M.; Krzemińska, I. Effectiveness of *Parachlorella kessleri* cell disruption evaluated with the use of laser light scattering methods. *J. Appl. Phycol.* **2019**, *31*, 97–107. [\[CrossRef\]](#)
31. Postma, P.R.; Miron, T.L.; Olivieri, G.; Barbosa, M.J.; Wijffels, R.H.; Eppink, M.H.M. Mild disintegration of the green microalgae *Chlorella vulgaris* using bead milling. *Bioresour. Technol.* **2015**, *184*, 297–304. [\[CrossRef\]](#) [\[PubMed\]](#)
32. Günerken, E.; D'Hondt, E.; Eppink, M.; Elst, K.; Wijffels, R. Flow cytometry to estimate the cell disruption yield and biomass release of *Chlorella* sp. during bead milling. *Algal Res.* **2017**, *25*, 25–31. [\[CrossRef\]](#)

